Developmental Biology 448 (2019) 161–172

Contents lists available at ScienceDirect

Developmental Biology

journal homepage: www.elsevier.com/locate/developmentalbiology

# Non-centrosomal microtubule structures regulated by egg activation signaling contribute to cytoplasmic and cortical reorganization in the ascidian egg

Toshiyuki Goto, Kazumasa Kanda, Takahito Nishikata*

*Frontiers of Innovative Research in Science and Technology (FIRST), Konan University, Kobe, Hyogo 650-0047, Japan*

ARTICLE INFO

*Keywords:*
Axis determination
$Ca^{2+}$ signaling
Fertilization
Cytoskeleton
Signal transduction

ABSTRACT

In the first ascidian cell cycle, cytoplasmic and cortical reorganization is required for distributing maternal factors to their appropriate positions, resulting in the formation of the embryonic axis. This cytoplasmic reorganization is considered to depend on the cortical microfilament network in the first phase and on the sperm astral microtubule (MT) in the second phase. Recently, we described three novel MT structures: a deeply extended MT meshwork (DEM) in the entire subcortical region of the unfertilized egg, transiently accumulated MT fragments (TAF) in the vegetal pole, and a cortical MT array in the posterior vegetal cortex (CAMP). Particularly, our previous study showed CAMP to contribute to the movement of myoplasm. In addition, it is very similar to the parallel MT array, which appears during cortical rotation in *Xenopus* eggs. However, how these MT structures are organized is still unclear. Here, we investigated the relationship between the egg activation pathway and MT structures during the first ascidian cell cycle. First, we carefully analyzed cell cycle progression through meiosis I and II and the first mitosis, and successfully established a standard time table of cell cycle events. Using this time table as a reference, we precisely described the behavior of novel MT structures and revealed that it was closely correlated with cell cycle events. Moreover, pharmacological experiments supported the relationship between these MT structures and the signal transduction mechanisms that begin after fertilization, including $Ca^{2+}$ signaling, MPF signaling, and MEK/MAPK signaling. Especially, CAMP formation was directed by activities of cyclin-dependent kinases. As these MT structures are conserved, at least, within chordate group, we emphasize the importance of understanding the controlling mechanisms of MT dynamics, which is important for embryonic axis determination in the ascidian egg.

## 1. Introduction

Ascidians are chordates, and in their eggs, a unique cytoplasmic domain called myoplasm can be identified. The myoplasm was originally described by Conklin (1905) and is thought to contain maternal information responsible for muscle determination. The myoplasm consists of a mitochondria-rich cytoplasmic region and cortical endoplasmic reticulum (cER) region containing maternal mRNAs (*i.e.* Type I *postplasmic/PEM* RNAs; Yoshida et al., 1996; Roegiers et al., 1999; Sardet et al., 2003; Paix et al., 2009; Makabe and Nishida, 2012), including that of the muscle determinant macho-1 (Nishida and Sawada, 2001). The myoplasm relocates toward the future posterior side by two phases of cytoplasmic and cortical reorganization during the first cell cycle (Roegiers et al., 1999; Sardet et al., 2007). The first phase of reorganization is actin-dependent, during which the myoplasm localizes to the vegetal pole (Sawada and Schatten, 1989; Chiba et al., 1999; Roegiers et al., 1999), whereas the second phase of reorganization is microtubule (MT)-dependent (Sawada and Schatten, 1989; Chiba et al., 1999; Roegiers et al., 1999). During the second phase of reorganization, a matured sperm aster moves toward the equator along the posterior-vegetal cortex (Sawada and Schatten, 1988; Sardet et al., 1989; Chiba et al., 1999; Roegiers et al., 1999), and the myoplasm relocates to the future posterior side, thereby establishing the egg anteroposterior axis (Sardet et al., 2003; Prodon et al., 2007; Makabe and Nishida, 2012).

Similar to the ascidian cytoplasmic and cortical reorganization, axis determination by massive cytoplasmic movement, directed by cytoskeletal filaments, has also been recognized in other animals (Elinson and Rowing, 1988; Houliston and Elinson, 1992; Abraham et al., 1995; Jesuthasan and Strähle, 1997; Elinson and Ninomiya, 2003; Tran et al., 2012). For example, during the first cell cycle in frogs, a highly aligned cortical MT array appears in the vegetal cortex followed by a

* Correspondence to: 7-1-20 Minatojima-minamimachi, Chuo-ku, Kobe 605-0047, Japan.
*E-mail address:* nisikata@konan-u.ac.jp (T. Nishikata).

https://doi.org/10.1016/j.ydbio.2018.10.014
Received 30 May 2018; Received in revised form 10 October 2018; Accepted 17 October 2018
Available online 26 October 2018

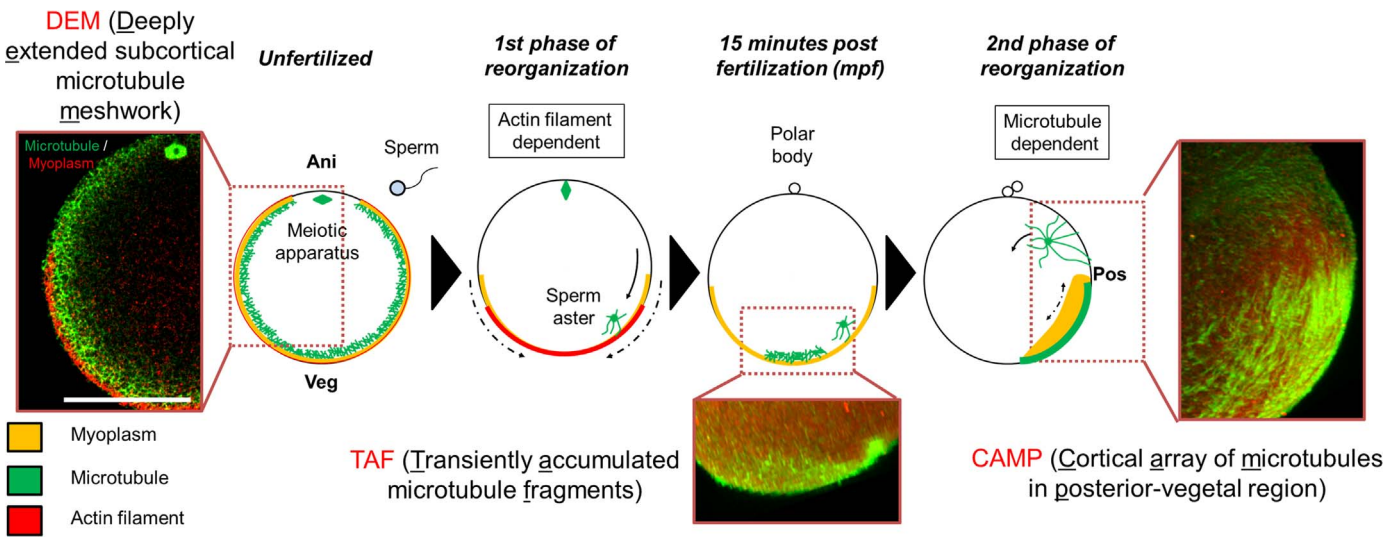


**Fig. 1.** Novel microtubule (MT) structures in cytoplasmic and cortical reorganization. Schematic drawing of cytoplasmic and cortical reorganization. In ascidian eggs, cytoplasmic and cortical reorganization have pivotal roles for the translocation of myoplasm (yellow), and actin filaments (red) and MTs (green) drive these movements. Photographs represent novel MT structures (red rectangles; DEM, TAF, and CAMP: Ishii et al., 2017). Embryos were stained for MT (green) and myoplasm (red), which was detected by the mitochondrial marker, anti-MnSOD antisera, because the myoplasm is mitochondria-rich. Scale bar, 50 μm.

type of cytoplasmic movement called cortical rotation. Concomitantly, maternal dorsalizing components (including *wnt11* mRNA and Dishevelled protein) translocate to the dorsal equatorial region followed by activation of the Wnt dorsalization pathway at the prospective dorsal side (Elinson and Rowning, 1988; Houliston and Elinson, 1992; Miller et al., 1999; Elinson and Ninomiya, 2003; Tao et al., 2005; Acosta et al., 2011). In addition to the cortical MT array, various MT structures play a role in the first cell cycle of these animal eggs (Houliston and Elinson, 1991; Abraham et al., 1995; Tran et al., 2012).

Previously, we reported three novel MT structures involved in the first cell cycle in ascidians by using modified Scale reagent G1T0 containing 4 M urea and 10 mM glycerol, but lacking Triton X-100, which enabled the visualization of obvious cortical MT structures (Fig. 1A; Ishii et al., 2017); namely, a deeply extended MT meshwork (DEM) in the entire subcortical region of an unfertilized egg, transiently accumulated MT fragments (TAF) at the vegetal pole, and a cortical MT array in the posterior vegetal cortex (CAMP). These structures differ from typical MT structures such as the mitotic apparatus in some aspects. For example, these structures are non-centrosomal and their shapes are heterogeneous. Especially, CAMP is similar to the cortical array of MTs during cortical rotation in frog eggs and it is also suggested to play a pivotal role in axis determination (Ishii et al., 2017). Despite the importance of these unique cytoskeletal structures in morphogenesis, limited information is available about their regulatory mechanisms.

On the other hand, the egg activation pathway, which is initiated by fertilization, has been examined relatively intensively in biochemical and cell biological studies. Early and late blocks to polyspermy, calcium wave and oscillation, and meiosis resumption are well-known phenomena in egg activation. These processes are regulated by signal transduction downstream to the putative sperm receptor (Becker and Hart, 1999; Dumollard et al., 2004; Ducibella and Fissore, 2007; Sensui et al., 2012; Levasseur et al., 2013; Tokmakov et al., 2014). Before fertilization, meiosis is arrested at various stages depending on the species (Whitaker, 1996; Hoshino et al., 2010). In mature ascidian oocytes, meiosis is arrested at Metaphase I by high activity of the cyclin-dependent kinase 1 (CDK1)/cyclin B complex (MPF) (Russo et al., 1996; Levasseur and McDougall, 2000; Sensui et al., 2012). In addition, high MPF activity is maintained by the mitogen-activated protein (MAP) pathway (Dumollard et al., 2011; Levasseur et al., 2013). After fertilization, a transient intracellular $Ca^{2+}$ rise is triggered by inositol 1,4,5-trisphosphate (IP3)-mediated release from the ER and the influx *via* $Ca^{2+}$ channels localized at plasma membrane (Yoshida et al., 1998; Dumollard et al., 2004). In an ascidian egg, two intracellular $Ca^{2+}$ rises followed by a series of $Ca^{2+}$ oscillations were reported just after fertilization (series I) and between the first and second polar body extrusions (series II) (Russo et al., 1996; Yoshida et al., 1998). Series I $Ca^{2+}$ oscillation causes Cyclin B destruction, leading to meiosis resumption (Levasseur et al., 2013). After extrusion of the first polar body, MPF activity increases to ensure entry into meiosis II and then decreases for extrusion of the second polar body (Russo et al., 1996; McDougall and Levasseur, 1998; Levasseur et al., 2013). MAP kinase (MAPK) activity also decreases during the second polar body extrusion (McDougall and Levasseur, 1998; Sensui et al., 2012).

It was recently reported in mouse and *Xenopus* oocytes that regulation of the meiotic apparatus, including spindle assembly and stabilization, is also affected by $Ca^{2+}$, MPF, and MAP kinase signaling pathways (Lefebvre et al., 2002; Bennabi et al., 2016; Li et al., 2016). In addition, *in vitro* and *in vivo* studies have revealed that many MT-interacting proteins could be substrates of these signaling molecules (Correas et al., 1992; Errico et al., 2010; Callender and Newton, 2017). Although the idea that MT structures during the first cell cycle are under control of egg activation pathway is largely applicable, the mechanisms that control cytoskeletal structures during the first cell cycle remain unresolved.

In this study, we investigated the relationship between egg activation pathway and MT structures during the first cell cycle in ascidians. First, we carefully analyzed cell cycle progression, *i.e.*, meiosis I and II and the first mitosis, and successfully established a standard time table of cell cycle events. Using this time table as a reference, we precisely described the behavior of novel MT structures and revealed that it was closely correlated with cell cycle events. Moreover, pharmacological experiments showed that these MT structures were regulated in accordance with the cell cycle progression, which is controlled by signal transduction mechanisms after fertilization, including $Ca^{2+}$ signaling, MPF signaling, and MEK/MAPK signaling. As these structures have pivotal roles for cytoplasmic and cortical reorganization, revealing the controlling mechanism of MT structures are important for understanding the fundamental developmental system of ascidians.

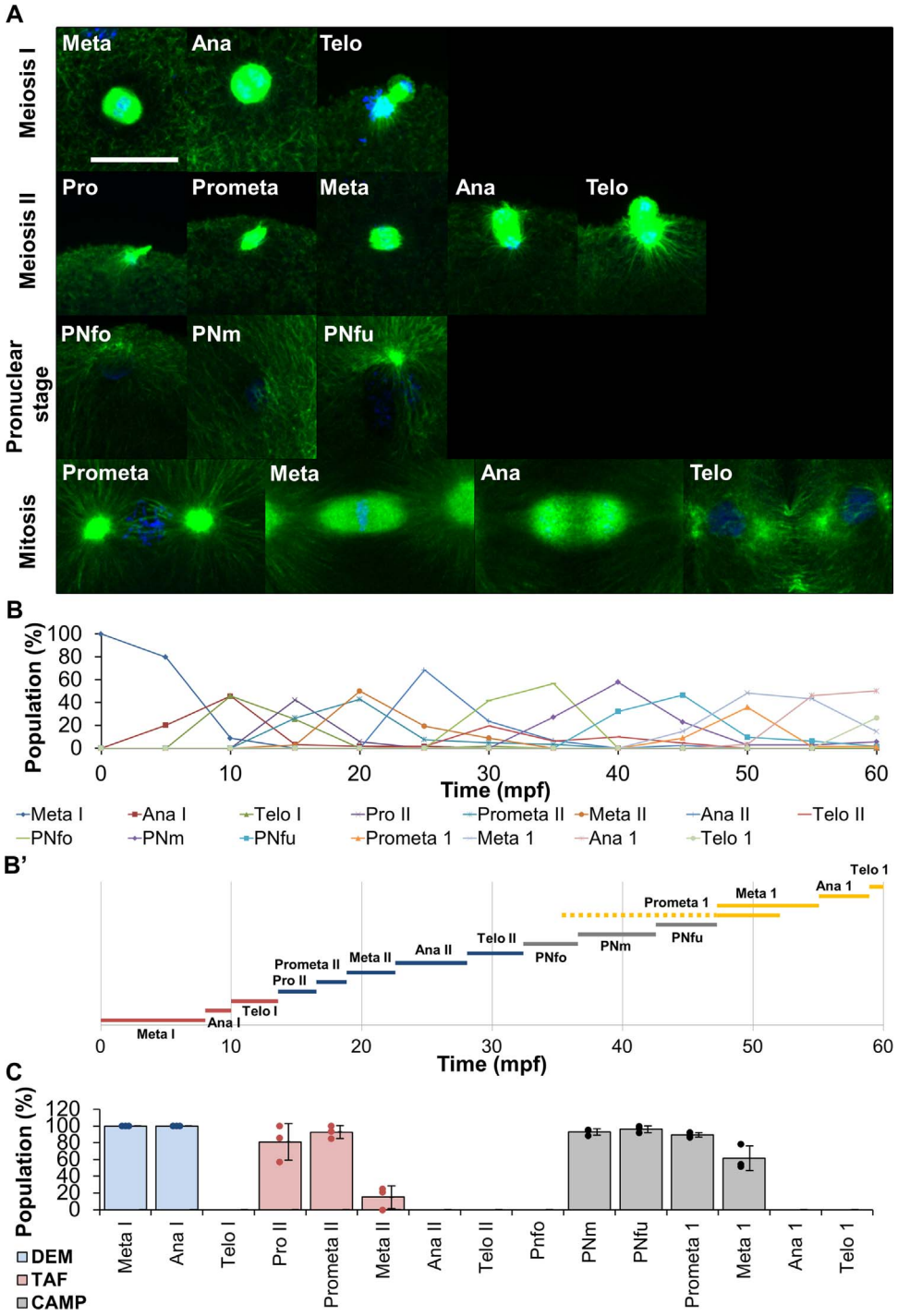


**Fig. 2.** Changes of microtubule (MT) structures during the first cell cycle. (A) Changes of meiotic and mitotic apparatuses and the nucleus during the first cell cycle in a fertilized *Ciona intestinalis* egg. Embryos were fixed at various stages and stained for MT (green) and chromatin (blue). Three-dimensional (3D) models rendered from confocal images are shown. Scale bar, 20 μm. (B, B') Progression of meiotic and mitotic cell cycle events were quantitatively analyzed and the duration of each event was estimated. PNfo, PNm, PNfu, and the suffix 1 denote pronuclear formation, pronuclear migration, pronuclear fusion, and mitosis of the first cell cycle, respectively. Three independent experiments were carried out and in total, more than 60 embryos were analyzed at each time point. Error bars represent standard deviation (SD; n = 3). Dotted line of Prometa 1 in B' indicates duplicated sperm centrosomes. (C) The concurrence of cell cycle events and novel MT structures was quantitatively analyzed. The population of embryos that showed each novel MT structure in each embryo stage were indicated. The experiment was the same as that described in B. At least 30 embryos were counted in each stage. Error bars represent SDs (n = 3) and the average of each experiment is represented as a dot.

## 2. Materials and methods

### 2.1. Embryos

Ascidian (*Ciona intestinalis* Type A; also called *Ciona robusta*) adults were provided by the National Bio-Resource Project (NBRP), Japan. Methods for handling egg and sperm, dechorionation, and fertilization were described previously (Ishii et al., 2012, 2014). Embryos were reared in filtered seawater at 18 °C. At this temperature, the first and second reorganization occur immediately after fertilization and about 30 min post-fertilization (mpf), respectively, and the first cleavage occurs around 60 mpf.

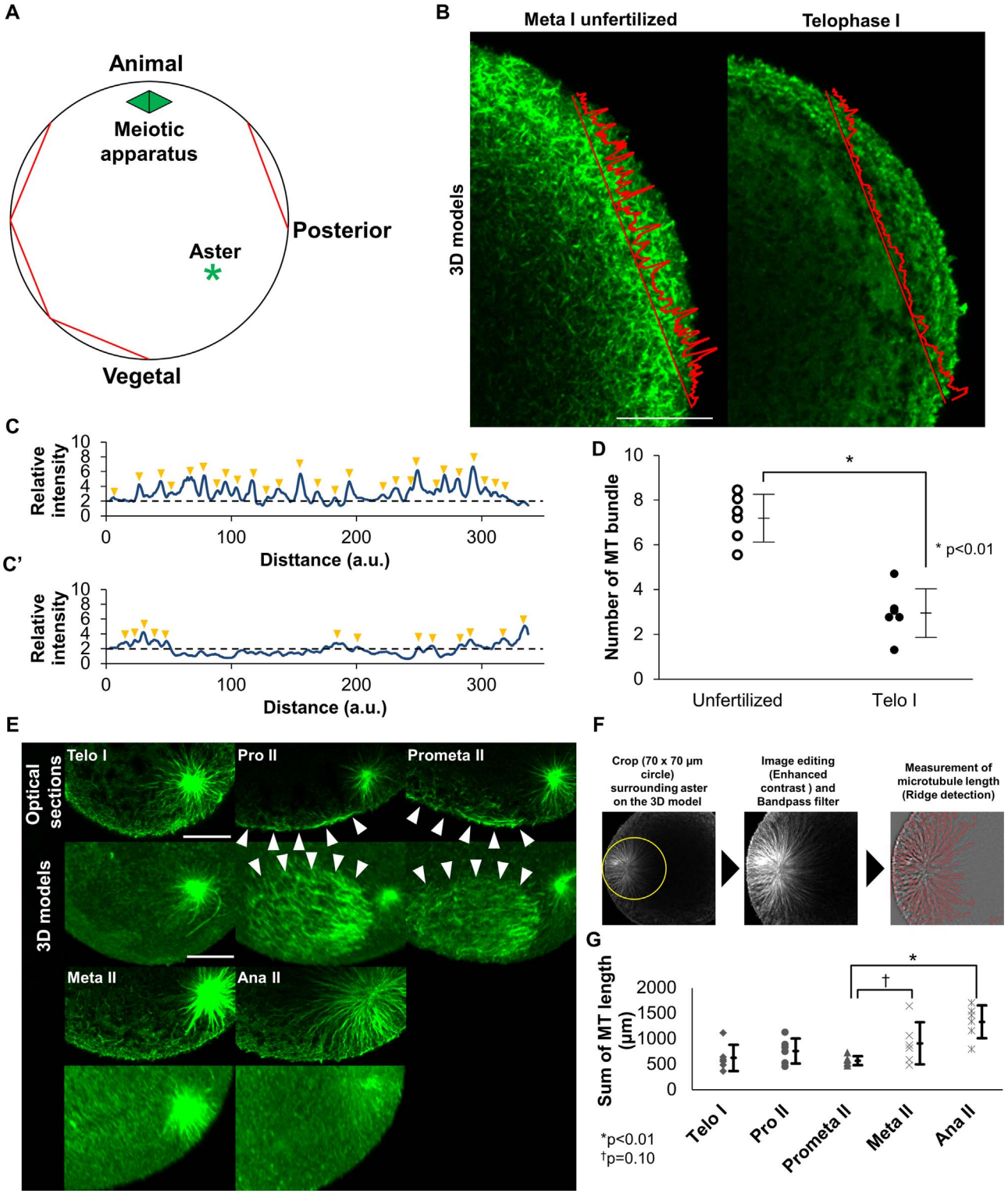


**Fig. 3.** Changes of deeply extended microtubule (MT) meshwork (DEM) and transiently accumulated fragments (TAF) along with meiotic progression. (A) Scheme for counting the number of MT fibers in the cortical meshwork. A regular octagon inscribed inside the egg cortex is drawn. Among this octagon, only 4 sides (chords; red lines), which do not interact with the meiotic apparatus or sperm aster are selected. Tubulin staining intensity along the selected chord is measured and the peaks in line profile of each chord are recognized as MT fibers. Such analysis was performed on 5 optical sections around mid-plane. (B) Embryos were stained for MT and the equatorial region of the mid-plane of the rendered 3D model is shown. Red line indicates an example of line profiling for tubulin staining. Scale bar, 20 µm. (C, C') Graphs show examples of line profiling of MT staining. C and C' are unfertilized egg and Telo I embryo, respectively. Line profiling was represented by relative intensities, which were normalized to the median of the entire egg and smoothened by moving average. The peak of the profile above the relative intensity value of 2.0 was recognized as an individual MT fiber (yellow arrow heads). (D) Dot plots show average number of MT fibers in each egg (n = 120: 4 chords on the 5 sections in 6 eggs). Significance was evaluated by a two-tailed *T*-test (*p < 0.01). (E) Changes of sperm aster and TAF (arrowheads) were observed in the mid-plane optical section and vegetal view of the 3D model (transparent). Note that the sperm aster seemed to start expansion in Meta II, when the TAF disappeared, and formed a significantly large well-developed sperm aster in Ana II. Scale bar, 20 µm. (F) Procedures for quantifying total MT length in the sperm aster. Six serial-optical sections containing the sperm aster were selected from confocal images and rendered 3D model. The sperm aster region was cropped to a 70-µm diameter circle. The image was edited to enhance microtubule bundles by the contrast enhancement and bandpass filter. Image J plugin "Ridge detection" (Steger, 1998) was applied to the edited image. (G) Sum of MT length in each stage is shown in dot plots with error bars (SD; n = 6). Significance was evaluated by two-tailed *T*-test (*p < 0.01, †p = 0.07 *versus* Ana II).

### 2.2. Pharmacological experiments

The final concentrations of calcium ionophore A23187 (CaI), cytochalasin B (CytB), U0126 (Sigma-Aldrich), and roscovitine (Merck) were 8 μM, 2 μg/ml, 1 μM, and 20 μM, respectively. Cycloheximide (Sigma-Aldrich) was used in two concentrations: 1 and 0.4 mM. In each experiment, the same dilution of each solvent (DMSO or ethanol) in filtered seawater was used as a control (Ctr). In unfertilized ascidian eggs, CaI treatment induces egg activation processes such as egg contraction and extrusion of the first polar body by the influx of external $Ca^{2+}$ (Sawada and Schatten, 1988).

### 2.3. Immunostaining

Whole *Ciona* embryos were fixed with 100% methanol, then treated with 100% ethanol. Fixed specimens were washed with phosphate-buffered saline containing 0.05% Tween 20 (PBST), then treated with G1T0 containing 4 mol/L urea (MP Biomedicals), and 1% glycerol in distilled water (Ishii et al., 2017) for 90 min at 4 °C, followed by a wash with PBST. After G1T0 treatment, specimens were stained with the following antibodies: anti-α-tubulin mouse monoclonal antibody (anti-MT; T9026 clone DM1A; Sigma-Aldrich; 1:100 dilution), anti-MnSOD rabbit antisera (anti-manganese superoxide dismutase; SPC-117C/D; StressMarq Biosciences; 1:40 dilution), Alexa Fluor 488-conjugated goat anti-mouse IgG antibody (A11001; Molecular Probes; 1:1000 dilution), and Alexa Fluor 532-conjugated goat anti-rabbit IgG antibody (A11009; Molecular Probes; 1:1000 dilution). The anti-MnSOD antisera is a good marker for the myoplasm because the myoplasm is rich in mitochondria (*e.g.* Ishii et al., 2012). Nuclei were stained with 5 μg/ml 4', 6-Diamidino-2-phenylindole dihydrochloride (DAPI). Stained specimens were mounted with methyl salicylate (Nacalai Tesque).

### 2.4. Image acquisition and data analysis

Specimens were observed under a LSM700 confocal microscope (Carl Zeiss). Three-dimensional images were rendered from confocal images and mid-plane images were generated in ZEN (Carl Zeiss). Three-dimensional (3D) models were displayed as a side view wherein vertical and crosswise directions correspond to the animal-vegetal and anterior-posterior axis, respectively, or as a posterior view in a rotated posterior direction. All analyses were performed in ImageJ Fiji (Schindelin et al., 2012). Quantification of characteristic features of MT structures are explained in Fig. 3.

## 3. Results

### 3.1. Novel MT structures and cell cycle events during the first cell cycle

Although we had already described three novel MT structures (Fig. 1A: Ishii et al., 2017), the timings of their appearance and disappearance were roughly identified as mpf, which is largely affected by the lag between insemination and establishment of fertilization. More accurate descriptions of these MT structures are needed to analyze their detailed regulatory mechanism.

To make a standard time table of progression of the first cell cycle, the meiotic and mitotic apparatus and chromosome, which can be detected simultaneously with the novel MT structures in the specimens stained for MTs, are preferable indicators of cell cycle events. The embryos were fixed every 5 min after insemination (though the results were described as mpf) and the cell cycle stage was determined according to the shape of spindle and nucleus (Fig. 2A). Note that the moving female pronucleus, just before nuclear fusion, had no obvious MT structure. As shown in Fig. 2B, the cell cycle stages clearly appear and disappear periodically. The period of these stages was determined as the duration of the stage that was most frequently observed in the population (Fig. 2B'). Notably, although the prometaphase and metaphase spindle of mitosis was established after pronuclear fusion, the centriole of sperm aster had already divided around 35 mpf (dotted yellow line of Fig. 2B'). Then, the populations of embryos that showed each MT structure in each staged embryo were analyzed. The results are summarized in Fig. 2C. The appearance and disappearance of these novel MT structures were consistent with the transition of the cell cycle stage. DEM disappeared in accordance with the transition from anaphase (Ana) I to telophase (Telo) I, TAF accumulated during prophase (Pro) II and prometaphase (Prometa) II, and CAMP could be observed from pronuclear migration (PNm) to metaphase of the first mitosis (Meta 1). These correlations suggested that there is some interaction between mechanisms of cell cycle progression and formation of MT structures.

### 3.2. Detailed observations of DEM and TAF

Subcortical regions of unfertilized eggs and Telo I embryos were compared (Fig. 3A). In unfertilized eggs, relatively thick MT bundles were randomly extended and formed a coarse meshwork (DEM). In the Telo I embryo, although the subcortical region had relatively bright staining, which made a gradient along the radius, few MT bundles could be observed. Quantitative analyses of these staining patterns showed clear decrease of MT fragments, indicating breakdown of the DEM (Fig. 3D).

In the vegetal hemisphere, sperm asters did not obviously change from Telo I to Prometa II and gradually developed starting from metaphase (Meta) II (Fig. 3E). Quantitative analysis of the total length of MTs in sperm asters confirmed the expansion of sperm asters during Meta II and Ana II (Fig. 3G). On the other hand, in the vegetal cortex, randomly oriented MT fragments gradually accumulated in Pro II and they were clearly visible in Prometa II as TAF, which later disappeared in Meta II (Figs. 3E, 3D model). The timing of the disappearance of TAF coincided with the expansion of sperm aster, which showed dynamic changes of its structure and position in the vegetal hemisphere during this period.

### 3.3. Detailed observations of CAMP formation

During the second phase of cytoplasmic and cortical reorganization, the well-developed sperm asters moved along the posterior vegetal cortex and reached the central region of the egg (Fig. 4). At the pronuclear formation (PNfo) stage, sperm asters were still in the vegetal hemisphere and some astral MTs reached the posterior cortex with bright foci. At the PNm stage, sperm asters reached the equatorial region. The MT foci on the vegetal cortex gradually formed a coarse network. This network might represent a premature form of CAMP. At the pronuclear fusion (PNfu) stage, sperm asters moved up to the animal hemisphere and the cortical MT bundles became thick and formed a parallel array, which is the characteristic feature of CAMP. At prometaphase of the first mitosis (Prometa 1) stage, sperm asters started to move inward and the parallel MT bundles in CAMP became disordered and tangled, suggesting a slow shrinkage of CAMP. At the Meta 1 stage, centrally positioned sperm asters had already divided and formed a bipolar metaphase spindle. It was confirmed that CAMP drastically shortened near the equatorial region (Ishii et al., 2017).

### 3.4. Control mechanisms of DEM and TAF

To reveal the regulatory mechanisms for the DEM and TAF, we focused on the relatively early mechanisms of the egg activation pathway such as $Ca^{2+}$ signaling. Treating unfertilized ascidian eggs with calcium ionophore A23187 (CaI) can mimic fertilization, and most of the events of egg activation, including $Ca^{2+}$ influx, $Ca^{2+}$ wave, the first phase of cortical reorganization, and resumption of meiosis can

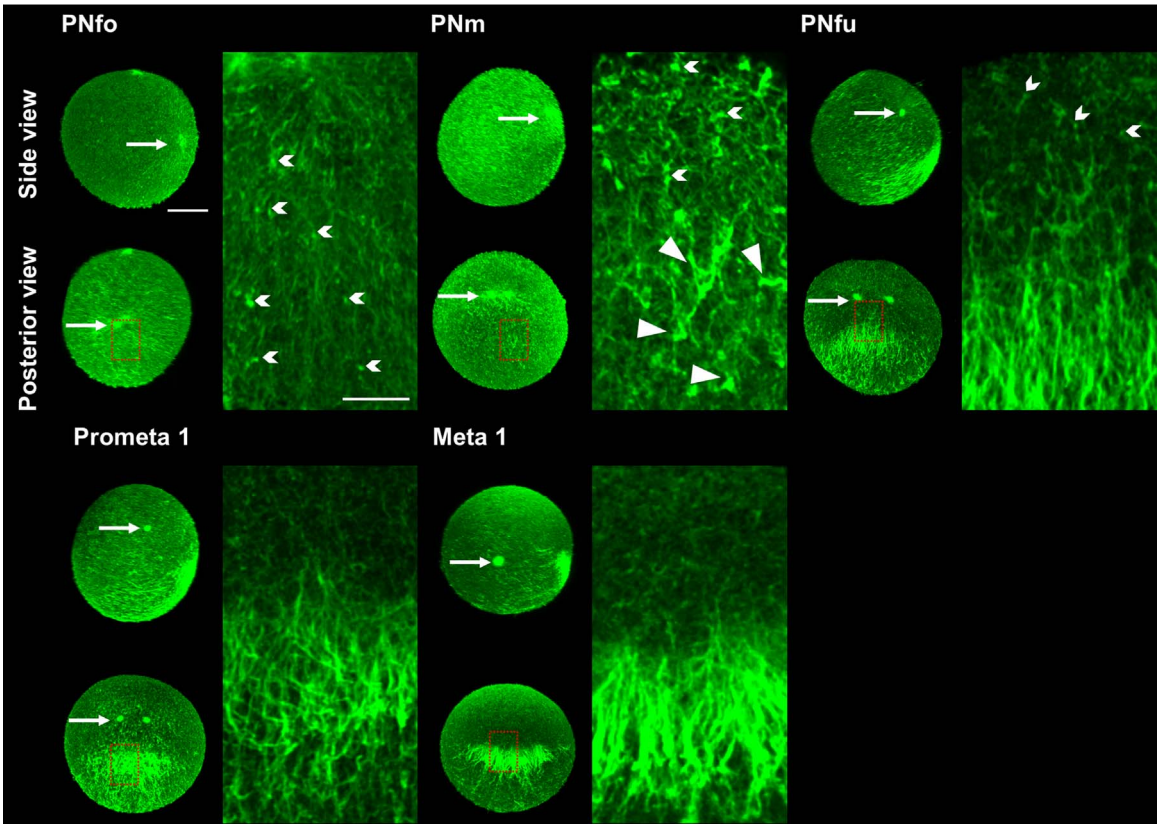


**Fig. 4.** Changes of sperm aster and cortical MT array in the posterior vegetal cortex (CAMP) during the pronuclear stage and mitosis. Embryos were stained for microtubules (MT) and the low-magnification 3D models are shown (left). Upper and lower images are side view and posterior view, respectively. Enlarged images of the red rectangle in left image are shown (right). Arrow, small arrow heads, and arrowhead indicate the sperm aster, attached point of astral MT to the cortex, and cortical MT focus, respectively. Scale bars, 50 (left image) and 20 (right image) μm.

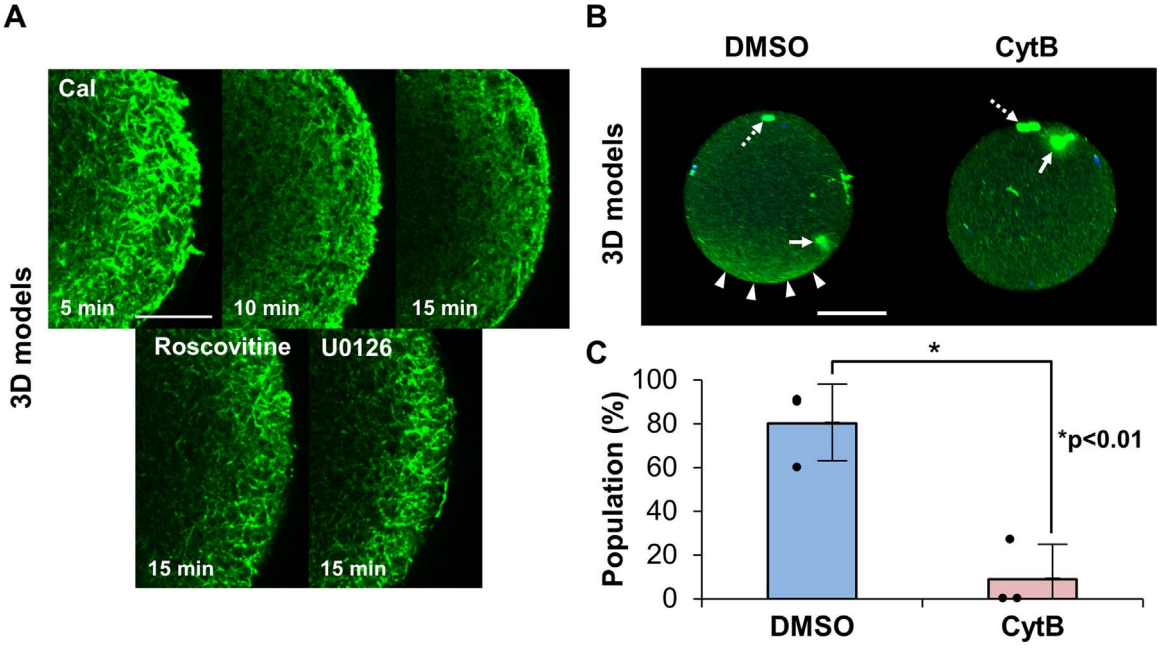


**Fig. 5.** The regulatory mechanisms of microtubule (MT) structures during meiosis. (A) Eggs activated with calcium ionophore A23187 (CaI, 8 μM) were reared with or without cell cycle inhibitors, roscovitine (20 μM) or U0126 (1 μM). Eggs were stained for MT and the mid-planes of the rendered 3D models are shown. The filamentous meshwork disappeared at 10 and 15 mpf upon CaI treatment, and no effect was observed in both inhibitor-treated embryos. Scale bar, 20 μm. (B) Unfertilized eggs were fertilized with or without cytochalasin B (CytB, 2 μg/ml) and reared until 20 mpf. Embryos were stained for MTs (green) and nuclei (blue), and the side view of 3D models are shown. Animal pole is up. In CytB-treated embryos, the prometaphase II female meiotic spindle (dotted arrow) became irregularly shaped owing to the inhibition of polar body extrusion, and the sperm aster (arrow) could not move to the vegetal hemisphere due to the inhibition of the first phase of reorganization. In addition, transiently accumulated fragments (TAFs) (arrowheads) could not be observed. Scale bar, 50 μm. (C) CytB- or DMSO-treated embryo, which showed TAF formation at Prophase II or Prometaphase II was counted in three independent experiments (more than 90 embryos in total). Error bars represent SDs (n = 3), and the average of each experiment is represented as a dot. Significance was evaluated by two-tailed *T*-test (*p < 0.01).

occur (Sawada and Schatten, 1988). In this experiment, CaI treatment induced the breakdown of DEM (Fig. 5A), while the U0126 (MEK inhibitor; Favata et al., 1998) and roscovitine (CDKs including CDK1, CDK2, and CDK5; Meijer et al., 1997), treatments did not induce DEM breakdown. These results suggested that, although the resumption of meiosis I is controlled by the rise in intracellular $Ca^{2+}$ concentration followed by the MAPK pathway and CDKs activities, the DEM breakdown could be controlled by the rise in intracellular $Ca^{2+}$ concentration but not be mediated by MAPK pathway and CDK activities.

Next, we focused on TAF accumulation. Although treating unfertilized eggs with CaI induced TAF accumulation (data not shown), we could not assess whether $Ca^{2+}$ signaling had a direct or indirect effect. Thus, we utilized cytochalasin B (CytB) treatment, which depolymerizes actin filaments and inhibits the first phase of cortical reorganization. As shown in Fig. 5B and C, although the timing of the first phase of rearrangement and the TAF accumulation were more than 10 min apart, CytB clearly inhibited the accumulation of TAF, revealing that TAF accumulation depended on the contraction of actin filaments. This result suggested that some interactions between the first phase of rearrangement and MT are required for proper organization of MT structure.

### 3.5. Control mechanisms of CAMP formation

In our experiment, when U0126 was treated from – 10 to 45 mpf, the female and male nuclei formed strange shapes and no CAMP was observed (Fig. 6A, B). Meanwhile, treatment between 30 and 45 mpf did not affect CAMP formation or meiotic and mitotic progression. Then, the effect of U0126 treatment was further analyzed in early stages of the cell cycle (Fig. 6C). At 10 mpf, control embryos showed a small sperm aster stick to the vegetal cortex, while in the treated embryos, the sperm aster had already largely expanded, resembling the shape of that observed in the Meta II stage around 20 mpf (cf Fig. 3E). At 20 mpf in the treated embryo, the female nucleus represented the PNfo stage consistent with the shape and position of sperm aster of PNfo stage around 35 mpf (cf Fig. 3E). At 30 mpf, a CAMP-like structure and the metaphase spindle were clearly observed clearly in the treated embryo, resembling those of the Meta 1 stage around 50 mpf. According to these results, the abolishment of CAMP in the U0126-treated embryo at 45 mpf did not represent an inhibition of CAMP formation, rather a precocious formation of CAMP.

However, a protein synthesis inhibitor, cycloheximide, can be used instead of U0126. In our experiment, when embryos were treated with 0.4 or 1.0 mM cycloheximide from -10 to 60 mpf, the CAMP were similar to those of 50 and 45 mpf embryos were formed, respectively (Fig. 6D). These results indicated that inhibiting protein synthesis caused a delay in CAMP formation and the behavior of sperm asters. The effects of both U0126 and cycloheximide treatments on CAMP formation will be discussed later.

### 3.6. Role of $Ca^{2+}$ signaling in CAMP formation

Next, we investigated the relationship between CAMP formation and $Ca^{2+}$ signaling. In ascidian eggs, $Ca^{2+}$ oscillation occurs in two phases (Russo et al., 1996; Sensui and Morisawa, 1996; Yoshida et al., 1998; Dumollard and Sardet, 2001; Sensui et al., 2012). The first and second series of oscillations correspond to meiosis I and II, respectively (Fig. 7A; Rosso et al., 1996; Dumollard and Sardet, 2001; Sensui et al., 2012). These $Ca^{2+}$ oscillations can be mimicked by CaI treatment or IP3 injection. Moreover, injection of adenophostin B, a nonmetaboliz-

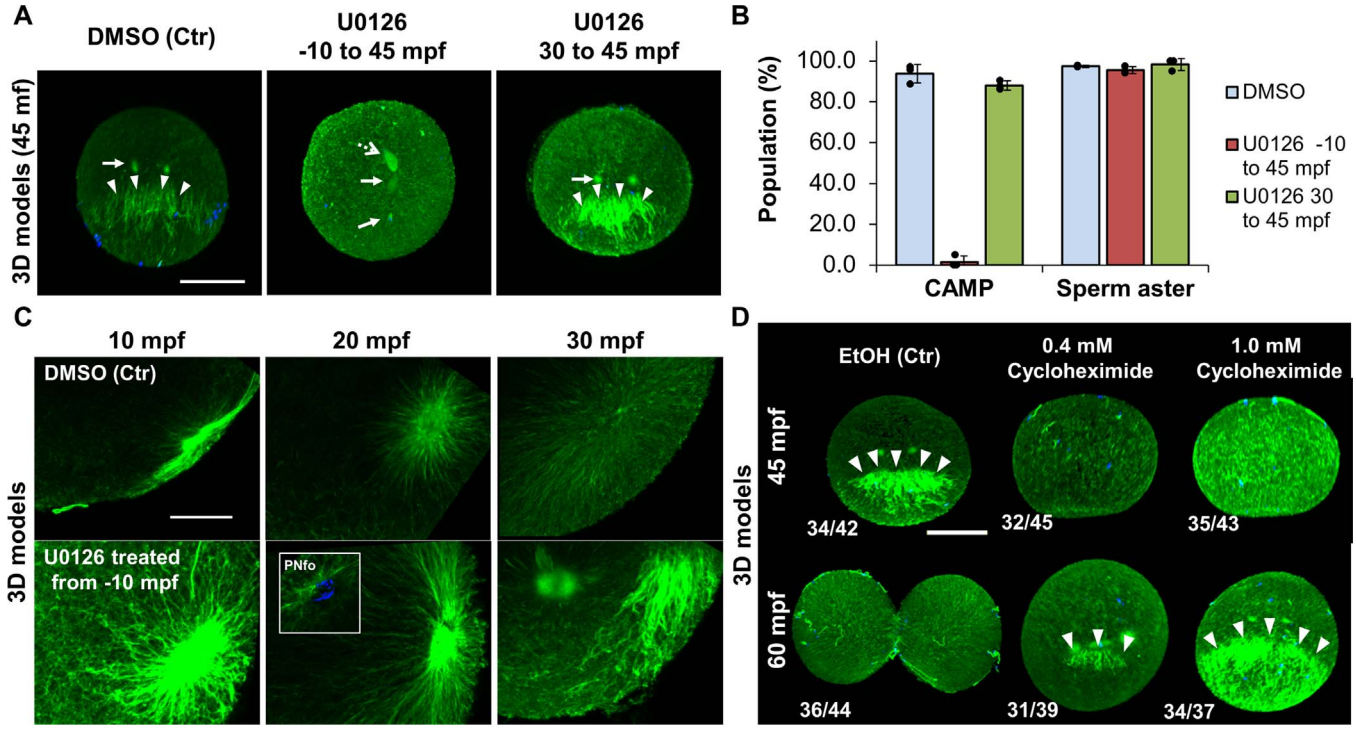


**Fig. 6.** Effects of U0126 on cortical microtubule (MT) array in the posterior vegetal cortex (CAMP) formation. (A) Embryos treated with U0126 (1 μM) during −10–45 or 30–45 mpf were fixed at 45 mpf and stained for MTs (green) and nuclei (blue). Posterior views of the 3D model rendered from confocal images are shown. Arrow, dotted arrow and arrowheads indicate sperm aster, meiotic apparatus, and CAMP, respectively. The centriole of the sperm aster had already divided at 45 mpf. Scale bar, 50 μm. (B) U0126- or DMSO-treated embryos, which contained CAMP or sperm asters were counted in three independent experiments (more than 100 embryos in total). Percentage of embryos, which had CAMP (left) or sperm aster (right) are shown in graph. Error bars represent SDs (n = 3), and the average of each experiment is represented as a dot. (C) Embryos treated with or without U0126 from -10 mpf were fixed in each time point and stained for MT. Rendered 3D models are shown. The white rectangle shows an enlarged image of the precociously formed female pronucleus. Scale bar, 20 μm. (D) Embryos were treated with cycloheximide (0.4 or 1.0 mM) from -10 to 45 or 60 mpf. Embryos were fixed at the end of these treatments and stained for MTs and nuclei. The posterior views of rendered 3D models are shown. Arrowheads indicate CAMP. The number of embryos, which showed a similar staining pattern to these photographs, in the total number of the specimens are indicated in the left corner. Scale bar, 50 μm.

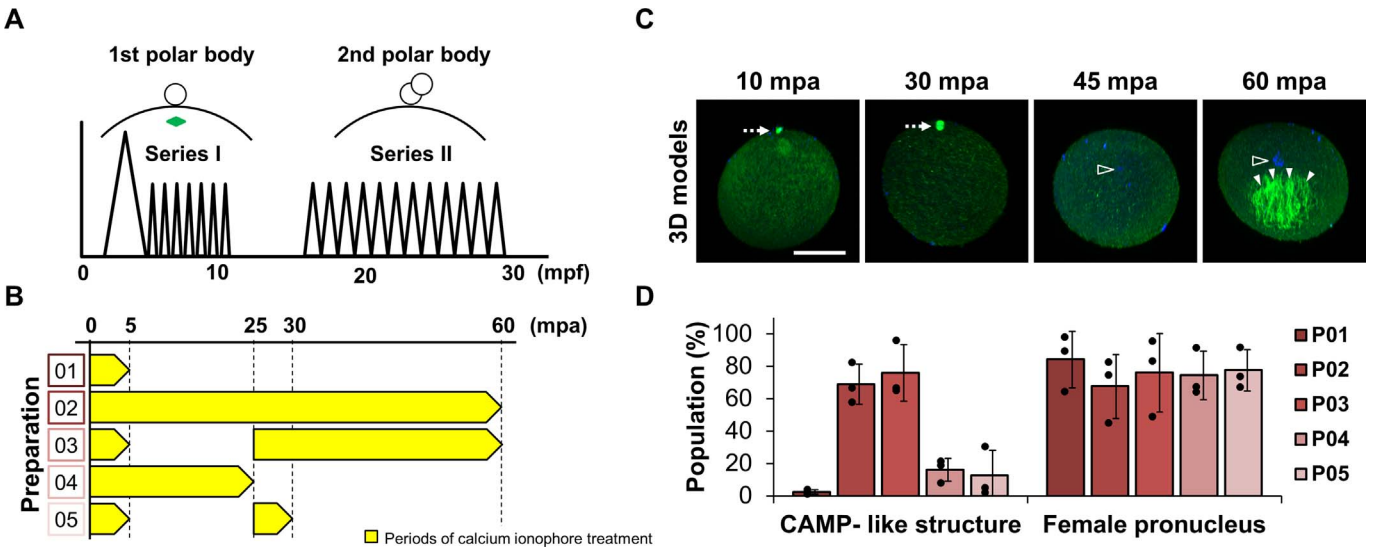


**Fig. 7.** Cortical MT array formation in the artificially activated egg. (A) Schematic drawing of two series of $Ca^{2+}$ oscillations and extrusion of two polar bodies in *Ciona intestinalis* revised from Russo et al. (1996). (B) Scheme of sample preparation (P01 to 05). The yellow blocks indicate incubation periods with CaI. (C) Unfertilized eggs were treated from 0 to 60 min with CaI (P02) and stained for MTs (green) and nuclei (blue). The 3D models rendered from confocal images were shown. Dotted arrow, open arrowhead, and arrowheads indicate meiotic apparatus, female pronucleus, and CAMP-like cortical MT array, respectively. Scale bar, 50 μm. (D) Percentage of activated eggs, which had CAMP-like structure (left) or female meiotic apparatus (right), were counted in three independent experiments (more than 100 embryos in total). Error bars represent SD (n = 3), and the average of each experiment is represented as a dot.

able agonist of the IP3 receptor, can induce continuous $Ca^{2+}$ oscillations up to 50 min post-activation (mpa) and extrusion of the second polar body (Yoshida et al., 1998). In order to reveal the relationship between CAMP formation and $Ca^{2+}$ oscillations, we designed a series of CaI treatments as shown in Fig. 7B. P01 (Sawada and Schatten, 1988) and P04 represent artificial activations by CaI mimicking fertilization and P02, which covered both first and second series of $Ca^{2+}$ oscillations, attempted to mimic the adenophostin B injection. As Yoshida et al. (1998) reported that serial IP3 injections with at least a 20-min interval could induce the first and second polar bodies and expected to induce the following pronuclear formation; P03 and P05 therefore have a 20-min interval.

The results showed that, for example in the embryos of the P02 preparation, the meiotic apparatus disappeared and a female pronucleus was formed with a small delay compared to the normal timing, and the formation of a CAMP-like structure was observed at 60 mpa (Fig. 7C). Quantitative analyses of CAMP-like structure and female pronucleus formation showed that while pronucleus formation was observed in all preparations, CAMP formation was achieved only in P02 and P03 (Fig. 7D). These results suggested that the first series of $Ca^{2+}$ oscillation, including the large $Ca^{2+}$ spike just after activation, is sufficient for resuming meiosis and starting mitosis, while $Ca^{2+}$ signaling in the pronuclear stage is important for CAMP formation.

### 3.7. CAMP formation and activities of CDKs

Finally, we analyzed whether activities of CDKs contribute to CAMP formation. CDKs are well-known cell cycle regulatory factors. In the first cell cycle in ascidians, MPF has three peaks of activity: at meiosis I and II and the first cleavage (Sensui et al., 2012). In order to reveal the relationship between CAMP formation and CDKs activities, we designed roscovitine treatments as shown in Fig. 8A to inhibit the activity of some CDKs. In control embryos, the CAMP and sperm aster formed normally (Fig. 8B; P06). However, all roscovitine-treated embryos did not exhibit CAMP formation (Fig. 8B, C; P07-P10) suggesting that CDK activity controls the CAMP formation.

In addition, although the meiotic apparatus was largely affected by roscovitine treatment, its effect on the mitotic apparatus and sperm aster were relatively small (Fig. 8B; arrows and dotted arrows). These differences are very important since the sperm aster and mitotic apparatus constitute the centrosomal MT structure. Centrosomal and non-centrosomal MT structures might be regulated differently by the egg activation pathway.

## 4. Discussion

We previously described three novel MT structures in ascidians during the first cell cycle in addition to meiotic and mitotic apparatuses and the sperm aster (Ishii et al., 2017). Here, we showed more detailed behavior of MT structures along with cell cycle progression and their relationship with the egg activation pathway (Fig. 9).

### 4.1. Breakdown of DEM after fertilization

In this study, we showed that the DEM in the cortical region of unfertilized eggs was broken down within 10 mpf and this breakdown was recapitulated by artificial egg activation with CaI treatment, but not by treatment with the CDK inhibitor roscovitine which probably inhibited MPF in this experiment, or treatment with the MEK inhibitor U0126 that thereby inhibits the MAPK pathway (Fig. 5A). In ascidian eggs, fertilization triggers $Ca^{2+}$ influx followed by the oscillation series I and the downregulation of MPF activity resulting in the resumption of meiosis (Russo et al., 1996; Yoshida et al., 1998). As it has been reported that $Ca^{2+}$ signaling induces MT destabilization (Correas et al., 1992; O'Brien et al., 1997; Callender and Newton, 2017), it is easy to deduce that $Ca^{2+}$ signaling controls DEM breakdown. Moreover, a similar MT network within the entire cytoplasm and its disappearance just after fertilization were also reported in *Xenopus* eggs (Houliston and Elinson, 1991), implying that such MT control after fertilization could be a conserved mechanism.

### 4.2. Vegetal accumulation of TAF during Pro and Prometa II

We also showed that contraction of the cortical actin network during the first phase of rearrangement contributes to the transient accumulation of MT fragment (TAF) at the vegetal pole cortex (Fig. 5B). This is the first example of the relationship between actin and tubulin cytoskeletal filaments during cytoplasmic rearrangement.

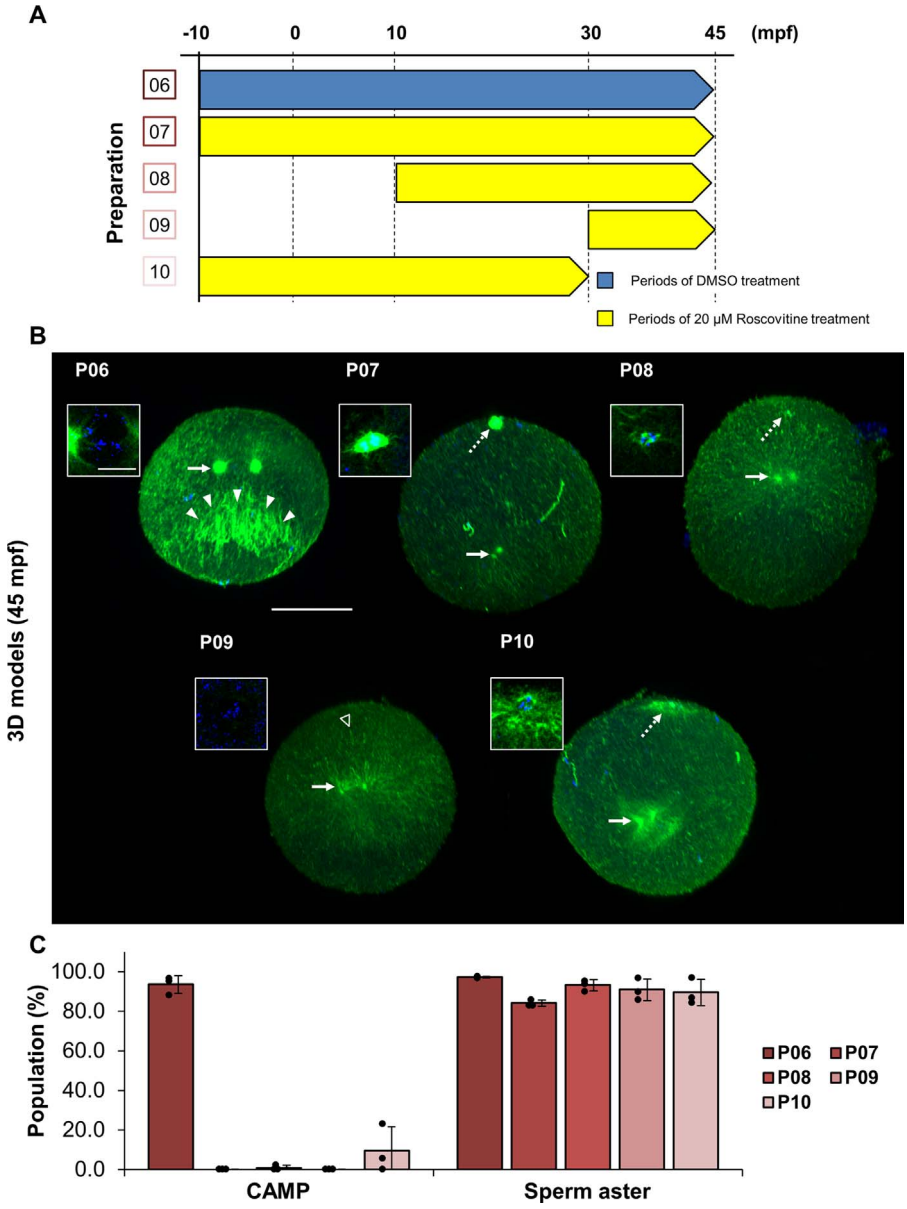


**Fig. 8.** Effect of roscovitine treatment on cortical microtubule (MT) array in the posterior vegetal cortex (CAMP) formation. (A) Scheme of sample preparation (P06 to 10). The blue and yellow blocks indicate incubation periods with DMSO and roscovitine (20 μM), respectively. (B) Embryos treated as indicated in A were fixed at 45 mpf and stained for MTs (green) and nuclei (blue). Posterior views of rendered 3D models are shown. Arrow, dotted arrow, open arrowhead, and arrowheads indicate sperm asters, meiotic apparatus, female pronucleus, and CAMP, respectively. The white rectangle shows an enlargement of fused (P06) and female (P07-P10) nuclei. Scale bars, 10 (within white rectangle) and 50 μm. (C) Roscovitine- or DMSO-treated embryos, containing CAMP or sperm aster were counted in three independent experiments (more than 90 embryos in total). The percentage of embryos containing CAMP (left) or sperm asters (right) are shown. Error bars represent SDs (n = 3), and the average of each experiment is represented as a dot.

As actin contraction occurred just after fertilization while the TAF accumulation occurred 15–20 mpf, the relationship between these two events is indirect. The myoplasm and cortical ER containing maternal mRNAs are segregated to the vegetal pole by actin contraction (Speksnijder et al., 1993; Roegiers et al., 1999; Chiba et al., 1999; Paix et al., 2009) and after that, they switch their transportation machinery from actin to tubulin, which is responsible for the second segregation. The relationship between actin contraction and TAF formation may contribute to this switch of the maternal information between cytoskeletal filaments.

### 4.3. Molecular mechanisms of CAMP formation

In normal *Ciona* development, MAPK activity remains high until the Telo I phase and gradually decreases until Telo II stage (Russo et al., 1996; McDougall and Levasseur, 1998). In this study, U0126 treatment starting from 30 mpf had no obvious effect on the embryo. This can be easily explained because the normal MAPK activity is low during this time. Meanwhile, U0126 treatment from -10 to 45 mpf resulted in unusual meiotic spindle and sperm aster in eccentric position. Similar results were reported by Sensui et al. (2012). They carried out a similar experiment and reported that the first polar body was extruded normally, but cytokinesis during the extrusion of the second polar body and the first cleavage was incomplete.

In this study, we further analyzed the early stage of the first cell cycle and clearly observed precocious CAMP formation and accelerated progression of meiosis and sperm aster movement (Fig. 6C). When unfertilized ascidian eggs were treated with U0126, the eggs were activated artificially, showing a precocious decrease of MAPK activity and giving rise to the progression of meiosis I followed by the entering into mitosis without extrusion of the second polar body (Dumollard et al., 2011). Moreover, other studies showed that in spoonworm

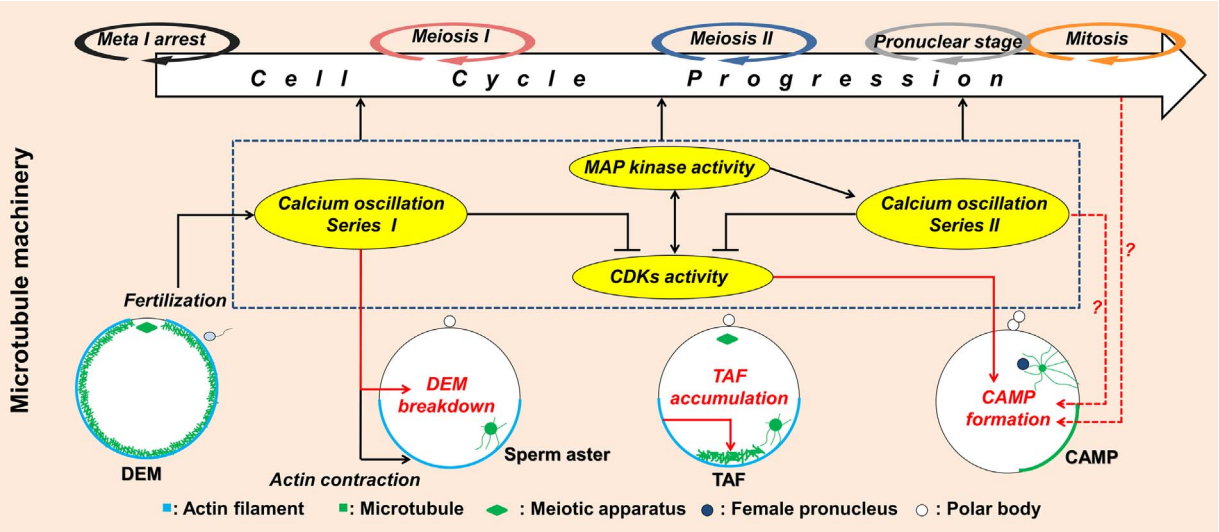


**Fig. 9.** Schematic model of the controlling mechanisms for microtubule (MT) structures during the first cell cycle in *Ciona intestinalis*. The egg activation pathway, including $Ca^{2+}$ signaling, MEK/MAPK signaling, and CDK1/Cyclin B (MPF) signaling, mutually regulate each other and direct cell cycle progression. MT structures including deeply extended MT meshwork (DEM), transiently accumulated MT fragments (TAF), and cortical MT array in the posterior vegetal cortex (CAMP), are regulated by the egg activation pathway concomitant with cell cycle progression. Red arrows indicate the novel regulatory mechanisms revealed in this study. Note that calcium signaling, actin contraction, and CDK activity regulate DEM breakdown, TAF formation, and CAMP formation, respectively. Dotted red lines represent processes that are still under debate.

| Reagent or resource | Source | Identifier |
|---|---|---|
| Antibodies | | |
| anti-α-tubulin mouse monoclonal antibody (clone DM1A) | Sigma-Aldrich | Cat#T9026 |
| anti-MnSOD rabbit antisera | StressMarq Biosciences | Cat#SPC-117C/D |
| Alexa Fluor 488-conjugated goat anti-mouse IgG antibody | Molecular Probes | Cat#A11001 |
| Alexa Fluor 532-conjugated goat anti-rabbit IgG antibody | Molecular Probes | Cat#A11009 |
| Bacterial and Virus Strains | | |
| Biological Samples | | |
| Chemicals, Peptides, and Recombinant Proteins | | |
| Calcium ionophore A23187 | Sigma-Aldrich | Cat#C-7522 |
| Cytochalasin B | Sigma-Aldrich | Cat#C-6762 |
| U0126 | Sigma-Aldrich | Cat#U120 |
| Roscovitine | Merck | Cat#557360 |
| Cycloheximide | Sigma-Aldrich | Cat#C-7698 |
| Urea | MP Biomedicals | Cat#821519 |
| methyl salicylate | Nacalai Tesque | Cat#23015–65 |
| Critical Commercial Assays | | |
| Deposited Data | | |
| Experimental Models: Cell Lines | | |
| Experimental Models: Organisms/Strains | | |
| *Ciona intestinalis*: wild type | National Bio-Resource Project | http://marinebio.nbrp.jp |
| Oligonucleotides | | |
| Recombinant DNA | | |
| Software and Algorithms | | |
| ZEN | Carl Zeiss | https:www.zeiss.com/microscopy/us/products/microscope-software/zen.html#introduction |
| ImageJ Fiji | Schindelin et al. (2012) | https://fiji.sc/ |
| Image J plugin “Ridge detection” | Steger (1998) | https://imagej.net/Ridge_Detection |
| Other | | |

(*Urechis caupo*), oyster (*Crassostrea gigas*), and starfish (*Asterina miniata*), inhibiting MAP kinase activity during the first cell cycle using U0126 induced premature sperm aster expansion similar to our observation (Gould and Stephano, 1999; Stephano and Gould, 2000; Fan and Sun, 2004). These reports support the idea that the down-regulating MAPK activity in fertilized eggs accelerates cell cycle progression. Thus, precocious formation of CAMP could be directed by this cell cycle acceleration. In contrast, a more direct effect of MAPK activity on CAMP formation can be also hypothesized. MAPK activity might suppress CAMP formation, and decreasing MAPK activity might trigger CAMP formation. In mouse oocytes, the metaphase II spindle is suggested to be maintained by the MAPK-interacting and spindle-stabilizing (MISS) protein *via* sustained MAPK activity (Lefebvre et al., 2002). Moreover, the mouse meiotic spindle is a non-centrosomal MT structure, suggesting a similar regulatory mechanism as that of CAMP formation.

On the other hand, we showed that inhibiting protein synthesis caused a delay in the CAMP formation and sperm aster movement (Fig. 6D). Previous studies also examined the effect of the protein synthesis inhibitor emetine (Marino et al., 2000; Russo et al., 2009). In

both reports, inhibiting protein synthesis in ascidian fertilized eggs suppressed reactivation of MPF activity around 30 mpf and kept high MAPK activity during the experimental period. As a result, second polar body formation and cleavage did not occur. These results were thought to be due to the blockage of cyclin B synthesis. However, cycloheximide and emetine inhibit protein synthesis non-specifically, suggesting that some proteins other than cyclin B could be candidates for regulating CAMP formation and the progression of cell cycle events.

### 4.4. Role of $Ca^{+}$ signaling in CAMP formation

In our study, the first large spike of $Ca^{2+}$ influx was sufficient to trigger the progression of meiosis, confirming results of previous studies (Russo et al., 1996; Sensui and Morisawa, 1996; Yoshida et al., 1998). However, this $Ca^{2+}$ spike was not sufficient to trigger CAMP formation; some unknown $Ca^{2+}$-related mechanism during the pronuclear stage was necessary for CAMP formation (Fig. 7). For the first series of $Ca^{2+}$ oscillation, it is widely accepted that calcineurin mediates the signal to the MPF activity through the anaphase-promoting complex/cyclosome (APC/C) (ex. Levasseur et al., 2013). Meanwhile, the mechanism of $Ca^{2+}$ signaling that controls MT structures is not well-studied. In *Xenopus* oocytes, Li et al. (2016) revealed that calmodulin localizes to the MTs and mediates the $Ca^{2+}$ signaling resulting in spindle formation. Thus, calmodulin is a possible mediator of CAMP formation.

### 4.5. Effect of CDK activity on CAMP formation

Using roscovitine treatment, we showed the importance of CDK activities for CAMP formation. Although the sperm centrosome was duplicated, suggesting the entry into the first mitotic phase, CAMP formation was completely abolished by roscovitine treatment, at least during the pronuclear stage (Fig. 8). In the first cell cycle, high levels of MPF activity appeared three times: in unfertilized eggs (meiotic metaphase I), before the second polar body extrusion (meiotic metaphase II), and before the first cleavage (first mitosis) (Sensui et al., 2012). According to this report, MPF activity was low during the pronuclear stage. However, in starfish embryos, a low level of MPF activity was inevitable for pronuclear formation during the first cell cycle (Tachibana et al., 2008). Moreover, in general, the interphase cyclin complex including the CDK2/Cyclin E complex and CDK1 or 2/Cyclin A complex exhibit high activity in G1 and S phases, respectively (Longo et al., 2008). Since roscovitine has a wide range of inhibitory effects on CDKs, including CDK1, 2, and 5 (Meijer et al., 1997), these results clearly support the idea that a relatively low level of CDK1 activity and/or other CDKs, including CDK2 and CDK5, positively regulate CAMP formation.

### 4.6. Importance of the control of MT dynamics

MTs are important structures for cytoplasmic and cortical rearrangement in ascidian development. Namely, they exert pivotal roles in morphogenesis, including localization of maternal factors, axis determination, and cell fate determination (Roegiers et al., 1999; Sasakura et al., 2000). Moreover, cortical MT arrays similar to the CAMP have also been recognized in frog eggs (Elinson and Rowning, 1988; Houliston and Elinson, 1992; Elinson and Ninomiya, 2003), and teleost eggs (Abraham et al., 1995; Jesuthasan and Strähle, 1997; Tran et al., 2012). These MT arrays also contribute to the large cytoplasmic relocation and axis determination by transporting dorsal determinants. The developmental system, in which such a cortical MT array and localized maternal factors function in the initial step of development, might be conserved within chordates.

In this study, we focused on the controlling mechanisms of three novel MT structures within the egg. It is a priori that these MT structures are controlled by egg activation signals beginning after fertilization, thus we could show some of which were related to the cell cycle control. Since, MTs are conserved in eukaryotic cells and the egg activation mechanisms are widely conserved in many species (*e.g.* Stricker, 1999; Roux et al., 2006; Ducibella and Fissore, 2007), the relationship between egg activation mechanisms and MT dynamics could be conserved in broader animal species.

Although interactions between different cytoskeletal filaments are reported by *in vitro* experiments (*e.g.* Waterman-Storer et al., 2000), little is known about details of the interaction between microfilaments and MTs, which is inevitable for the correct transport of cytoplasmic factors in ascidian eggs. As we clearly showed the novel relationship between microfilaments and MTs during TAF formation, it could be a clue for understanding the mechanisms of the rearrangement of maternal factors. Thus, revealing the entire mechanism of controlling MT structures will help us understand the basics of the initial developmental step in chordate eggs and shed light on the emergence and evolution of chordates.

## 5. Conclusion

In this study, we, for the first time, demonstrated the relationship between three novel MT structures and egg activation pathway during the first cell cycle in an ascidian *Ciona intestinalis*. 1) DEM, the cortical meshwork in unfertilized eggs, broke down in response to $Ca^{2+}$ signaling. 2) TAF, the vegetal accumulation of fragments at the end of meiosis, formed depending on the first cytoplasmic reorganization. 3) Formation of CAMP, a parallel array in the posterior vegetal cortex, could be controlled by CDK activities and some other mechanisms including $Ca^{2+}$ signaling. Since these MT structures are related to cytoplasmic and cortical reorganization, we emphasize the importance of understanding the controlling mechanisms of MT dynamics, which is important for embryonic axis determination in the ascidian egg.

## Acknowledgements

We would like to thank Dr. K. Tachibana (Tokyo Institute of Technology, Japan) for valuable discussion about egg activation signaling. We thank the National Bio-Resource Project for providing *Ciona intestinalis*. This research did not receive any specific grant from funding agencies in the public, commercial, or not-for-profit sectors.

## References

Abraham, V.C., Miller, A.L., Fluck, R.A., 1995. Microtubule arrays during ooplasmic segregation in the medaka fish egg (Oryzias latipes). Biol. Bull. 188, 136–145. http://dx.doi.org/10.2307/1542079.

Acosta, H., López, S.L., Revinski, D.R., Carrasco, A.E., 2011. Notch destabilises maternal beta-catenin and restricts dorsal-anterior development in Xenopus. Development 138, 2567–2579. http://dx.doi.org/10.1242/dev.061143.

Becker, K.A., Hart, N.H., 1999. Reorganization of filamentous actin and myosin-II in zebrafish eggs correlates temporally and spatially with cortical granule exocytosis. J. Cell Sci. 112, 97–110, (PMID: 9841907).

Bennabi, I., Terret, M.E., Verlhac, M.H., 2016. Meiotic spindle assembly and chromosome segregation in oocytes. J. Cell Biol. 215, 611–619. http://dx.doi.org/10.1083/jcb.201607062.

Callender, J.A., Newton, A.C., 2017. Conventional protein kinase C in the brain: 40 years later. Neuro Signal 1. http://dx.doi.org/10.1042/NS20160005, (NS20160005).

Chiba, S., Miki, Y., Ashida, K., Wada, M.R., Tanaka, K.J., Shibata, Y., Nakamori, R., Nishikata, T., 1999. Interactions between cytoskeletal components during myoplasm rearrangement in ascidian eggs. Dev. Growth Differ. 41, 265–272. http://dx.doi.org/10.1046/j.1440-169X.1999.413433.x.

Conklin, E.G., 1905. The organization and cell lineage of the ascidian egg. J. Acad. Nat. Sci. Phila. 13, 1–119.

Correas, I., Díaz-Nido, J., Avila, J., 1992. Microtubule-associated protein tau is phosphorylated by protein kinase C on its tubulin binding domain. J. Biol. Chem. 267, 15721–15728, (PMID: 1639808).

Ducibella, T., Fissore, R., 2007. The roles of Ca2+, downstream protein kinases, and oscillatory signaling in regulating fertilization and the activation of development. Dev. Biol. 315, 257–279. http://dx.doi.org/10.1016/j.ydbio.2007.12.012.

Dumollard, R., Sardet, C., 2001. Three different calcium wave pacemakers in ascidian eggs. J. Cell Sci. 114, 2471–2481, (PMID: 11559755).

Dumollard, R., McDougall, A., Rouvière, C., Sardet, C., 2004. Fertilisation calcium signals in the ascidian egg. Biol. Cell 96, 29–36. http://dx.doi.org/10.1016/j.biolcel.2003.11.002.

Dumollard, R., Levasseur, M., Hebras, C., Huitorel, P., Carroll, M., Chambon, J.P., McDougall, A., 2011. Mos limits the number of meiotic divisions in urochordate eggs. Development 138, 885–895. http://dx.doi.org/10.1242/dev.057133.
Elinson, R.P., Rowning, B., 1988. A transient array of parallel microtubules in frog eggs: potential tracks for a cytoplasmic rotation that specifies the dorso-ventral axis. Dev. Biol. 128, 185–197, (PMID: 3289985).
Elinson, R.P., Ninomiya, H., 2003. Parallel microtubules and other conserved elements of dorsal axial specification in the direct developing frog, Eleutherodactylus coqui. Dev. Genes Evol. 213, 28–34. http://dx.doi.org/10.1007/s00427-002-0290-8.
Errico, A., Deshmukh, K., Tanaka, Y., Pozniakovsky, A., Hunt, T., 2010. Identification of substrates for cyclin dependent kinases. Adv. Enzym. Regul. 50, 375–399. http://dx.doi.org/10.1016/j.advenzreg.2009.12.001.
Fan, H.Y., Sun, Q.Y., 2004. Involvement of mitogen-activated protein kinase cascade during oocyte maturation and fertilization in mammals. Biol. Reprod. 70, 535–547. http://dx.doi.org/10.1095/biolreprod.103.022830.
Favata, M.F., Horiuchi, K.Y., Manos, E.J., Daulerio, A.J., Stradley, D.A., Feeser, W.S., Van Dyk, D.E., Pitts, W.J., Earl, R.A., Hobbs, F., Copeland, R.A., Magolda, R.L., Scherle, P.A., Trzaskos, J.M., 1998. Identification of a novel inhibitor of mitogen-activated protein kinase kinase. J. Biol. Chem. 273, 18623–18632, (PMID: 9660836).
Gould, M.C., Stephano, J.L., 1999. MAP kinase, meiosis, and sperm centrosome suppression in Urechis caupo. Dev. Biol. 216, 348–358. http://dx.doi.org/10.1006/dbio.1999.9468.
Hoshino, Y., Sato, Y., Sakai, C., Sato, E., 2010. The signal transduction of meiotic progression in Mammalian Oocytes. J. Mamm. Ova Res. 27, 21–26. http://dx.doi.org/10.1274/jmor.27.21.
Houliston, E., Elinson, R.P., 1991. Patterns of microtubule polymerization relating to cortical rotation in Xenopus laevis eggs. Development 112, 107–117, (PMID: 1769322).
Houliston, E., Elinson, R.P., 1992. Microtubules and cytoplasmic reorganization in the frog egg. Curr. Top. Dev. Biol. 26, 53–70.
Ishii, H., Kunihiro, S., Tanaka, M., Hatano, K., Nishikata, T., 2012. Cytosolic subunits of ATP synthase are localized to the cortical endoplasmic reticulum-rich domain of the ascidian egg myoplasm. Dev. Growth Differ. 54, 753–766. http://dx.doi.org/10.1111/dgd.12003.
Ishii, H., Shirai, T., Makino, C., Nishikata, T., 2014. Mitochondrial inhibitor sodium azide inhibits the reorganization of mitochondria-rich cytoplasm and the establishment of the anteroposterior axis in ascidian embryo. Dev. Growth Differ. 56, 175–188. http://dx.doi.org/10.1111/dgd.12117.
Ishii, H., Goto, T., Nishikata, T., 2017. Microtubule array observed in the posterior-vegetal cortex during cytoplasmic and cortical reorganization of the ascidian egg. Dev. Growth Differ. 59, 648–656. http://dx.doi.org/10.1111/dgd.12405.
Jesuthasan, S., Strähle, U., 1997. Dynamic microtubules and specification of the zebrafish embryonic axis. Curr. Biol. 7, 31–42, (PMID: 9024620).
Lefebvre, C., Terret, M.E., Djiane, A., Rassinier, P., Maro, B., Verlhac, M.H., 2002. Meiotic spindle stability depends on MAPK-interacting and spindle-stabilizing protein (MISS), a new MAPK substrate. J. Cell Biol. 157, 603–613. http://dx.doi.org/10.1083/jcb.200202052.
Levasseur, M., McDougall, A., 2000. Sperm-induced calcium oscillations at fertilisation in ascidians are controlled by cyclin B1-dependent kinase activity. Development 127, 631–641, (PMID: 10631183).
Levasseur, M., Dumollard, R., Chambon, J.P., Hebras, C., Sinclair, M., Whitaker, M., McDougall, A., 2013. Release from meiotic arrest in ascidian eggs requires the activity of two phosphatases but not CaMKII. Development 140, 4583–4593. http://dx.doi.org/10.1242/dev.096578.
Li, R., Leblanc, J., He, K., Liu, X.J., 2016. Spindle function in Xenopus oocytes involves possible nanodomain calcium signaling. Mol. Biol. Cell 27, 3273–3283. http://dx.doi.org/10.1091/mbc.E16-05-0338.
Longo, V.D., Lieber, M.R., Vijg, J., 2008. Turning anti-ageing genes against cancer. Nat. Rev. Mol. Cell Biol. 9, 903–910. http://dx.doi.org/10.1038/nrm2526.
Makabe, K.W., Nishida, H., 2012. Cytoplasmic localization and reorganization in ascidian eggs: role of postplasmic/PEM RNAs in axis formation and fate determination. Rev. Dev. Biol. 1, 501–518. http://dx.doi.org/10.1002/wdev.54.
Marino, M., Wilding, M., Dale, B., 2000. Interaction of cell cycle kinases, microtubules, and chromatin in ascidian oocytes during meiosis. Mol. Reprod. Dev. 56, 155–162. http://dx.doi.org/10.1002/(SICI)1098-2795(200006)56:2<155::AID-MRD6>3.0.CO;2-1.
McDougall, A., Levasseur, M., 1998. Sperm-triggered calcium oscillations during meiosis in ascidian oocytes first pause, restart, then stop: correlations with cell cycle kinase activity. Development 125, 4451–4459, (PMID: 9778504).
Meijer, L., Borgne, A., Mulner, O., Chong, J.P., Blow, J.J., Inagaki, N., Inagaki, M., Delcros, J.G., Moulinoux, J.P., 1997. Biochemical and cellular effects of roscovitine, a potent and selective inhibitor of the cyclin-dependent kinases cdc2, cdk2 and cdk5. Eur. J. Biochem. 243, 527–536, (PMID: 9030781).
Miller, J.R., Rowning, B.A., Larabell, C.A., Yang-Snyder, J.A., Bates, R.L., Moon, R.T., 1999. Establishment of the dorsal-ventral axis in Xenopus embryos coincides with the dorsal enrichment of dishevelled that is dependent on cortical rotation. J. Cell Biol. 146, 427–437, (PMCID: PMC2156185).
Nishida, H., Sawada, K., 2001. macho-1 encodes a localized mRNA in ascidian eggs that specifies muscle fate during embryogenesis. Nature 409, 724–729. http://dx.doi.org/10.1038/35055568.
O'Brien, E.T., Salmon, E.D., Erickson, H.P., 1997. How calcium causes microtubule depolymerization. Cell Motil. Cytoskelet. 36, 125–135.
Paix, A., Yamada, L., Dru, P., Lecordier, H., Pruliere, G., Chenevert, J., Satoh, N., Sardet, C., 2009. Cortical anchorages and cell type segregations of maternal postplasmic/PEM RNAs in ascidians. Dev. Biol. 336, 96–111. http://dx.doi.org/10.1016/j.ydbio.2009.09.001.
Prodon, F., Yamada, L., Shirae-Kurabayashi, M., Nakamura, Y., Sasakura, Y., 2007. Postplasmic/PEM RNAs: a class of localized maternal mRNAs with multiple roles in cell polarity and development in ascidian embryos. Dev. Dyn. 236, 1698–1715. http://dx.doi.org/10.1002/dvdy.21109.
Roegiers, F., Djediat, C., Dumollard, R., Rouvière, C., Sardet, C., 1999. Phases of cytoplasmic and cortical reorganizations of the ascidian zygote between fertilization and first division. Development 126, 3101–3117, (PMID: 10375502).
Roux, M.M., Townley, I.K., Raisch, M., Reade, A., Bradham, C., Humphreys, G., Gunaratne, H.J., Killian, C.E., Moy, G., Su, Y.H., Ettensohn, C.A., Wilt, F., Vacquier, V.D., Burke, R.D., Wessel, G., Foltz, K.R., 2006. A functional genomic and proteomic perspective of sea urchin calcium signaling and egg activation. Dev. Biol. 300, 416–433. http://dx.doi.org/10.1016/j.ydbio.2006.09.006.
Russo, G.L., Kyozuka, K., Antonazzo, L., Tosti, E., Dale, B., 1996. Maturation promoting factor in ascidian oocytes is regulated by different intracellular signals at meiosis I and II. Development 122, 1995–2003, (PMID: 8681780).
Russo, G.L., Bilotto, S., Ciarcia, G., Tosti, E., 2009. Phylogenetic conservation of cytostatic factor related genes in the ascidian Ciona intestinalis. Gene 429, 104–111. http://dx.doi.org/10.1016/j.gene.2008.09.035.
Sardet, C., Speksnijder, J., Inoue, S., Jaffe, L., 1989. Fertilization and ooplasmic movements in the ascidian egg. Development 105, 237–249, (PMID: 2806123).
Sardet, C., Nishida, H., Prodon, F., Sawada, K., 2003. Maternal mRNAs of PEM and macho 1, the ascidian muscle determinant, associate and move with a rough endoplasmic reticulum network in the egg cortex. Development 130, 5839–5849. http://dx.doi.org/10.1242/dev.00805.
Sardet, C., Paix, A., Prodon, F., Dru, P., Chenevert, J., 2007. From oocyte to 16-cell stage: cytoplasmic and cortical reorganizations that pattern the ascidian embryo. Dev. Dyn. 236, 1716–1731. http://dx.doi.org/10.1002/dvdy.21136.
Sasakura, Y., Ogasawara, M., Makabe, K.W., 2000. Two pathways of maternal RNA localization at the posterior-vegetal cytoplasm in early ascidian embryos. Dev. Biol. 220, 365–378. http://dx.doi.org/10.1006/dbio.2000.9626.
Sawada, T., Schatten, G., 1988. Microtubules in ascidian eggs during meiosis, fertilization, and mitosis. Cell Motil. Cytoskelet. 9, 219–230. http://dx.doi.org/10.1002/cm.970090304.
Sawada, T., Schatten, G., 1989. Effects of cytoskeletal inhibitors on ooplasmic segregation and microtubule organization during fertilization and early development in the ascidian Molgula occidentalis. Dev. Biol. 132, 331–342, (PMID: 2466714).
Schindelin, J., Arganda-Carreras, I., Frise, E., Kaynig, V., Longair, M., Pietzsch, T., Preibisch, S., Rueden, C., Saalfeld, S., Schmid, B., Tinevez, J.Y., White, D.J., Hartenstein, V., Eliceiri, K., Tomancak, P., Cardona, A., 2012. Fiji: an open-source platform for biological-image analysis. Nat. Methods 9, 676–682. http://dx.doi.org/10.1038/nmeth.2019.
Sensui, N., Morisawa, M., 1996. Effect of Ca2+ on deformation, polar body extrusion and pronucleus formation in the egg of the ascidian. Ciona savignyi, Devl. Growth Differ. 38, 341–350. http://dx.doi.org/10.1046/j.1440-169X.1996.t01-3-00002.x.
Sensui, N., Yoshida, M., Tachibana, K., 2012. Role of Mos/MEK/ERK cascade and cdk1 in Ca2+ oscillations in fertilized ascidian eggs. Dev. Biol. 367, 208–215. http://dx.doi.org/10.1016/j.ydbio.2012.05.011.
Speksnijder, J.E., Terasaki, M., Hage, W.J., Jaffe, L.F., Sardet, C., 1993. Polarity and reorganization of the endoplasmic reticulum during fertilization and ooplasmic segregation in the ascidian egg. J. Cell Biol. 120, 1337–1346, (PMCID: PMC2119754).
Steger, C., 1998. An unbiased detector of curvilinear structures. IEEE Trans. Pattern Anal. Mach. Intell. 20, 113–125. http://dx.doi.org/10.1109/34.659930.
Stephano, J.L., Gould, M.C., 2000. MAP kinase, a universal suppressor of sperm centrosomes during meiosis? Dev. Biol. 222, 420–428. http://dx.doi.org/10.1006/dbio.2000.9726.
Stricker, S.A., 1999. Comparative biology of calcium signaling during fertilization and egg activation in animals. Dev. Biol. 211, 157–176. http://dx.doi.org/10.1006/dbio.1999.9340.
Tachibana, K., Hara, M., Hattori, Y., Kishimoto, T., 2008. Cyclin B-cdk1 controls pronuclear union in interphase. Curr. Biol. 18, 1308–1313. http://dx.doi.org/10.1016/j.cub.2008.07.077.
Tao, Q., Yokota, C., Puck, H., Kofron, M., Birsoy, B., Yan, D., Asashima, M., Wylie, C.C., Lin, X., Heasman, J., 2005. Maternal wnt11 activates the canonical wnt signaling pathway required for axis formation in Xenopus embryos. Cell 120, 857–871. http://dx.doi.org/10.1016/j.cell.2005.01.013.
Tokmakov, A.A., Stefanov, V.E., Iwasaki, T., Sato, K., Fukami, Y., 2014. Calcium signaling and meiotic exit at fertilization in Xenopus egg. Int. J. Mol. Sci. 15, 18659–18676. http://dx.doi.org/10.3390/ijms151018659.
Tran, L.D., Hino, H., Quach, H., Lim, S., Shindo, A., Mimori-Kiyosue, Y., Mione, M., Ueno, N., Winkler, C., Hibi, M., Sampath, K., 2012. Dynamic microtubules at the vegetal cortex predict the embryonic axis in zebrafish. Development 139, 3644–3652. http://dx.doi.org/10.1242/dev.082362.
Waterman-Storer, C., Duey, D.Y., Weber, K.L., Keech, J., Cheney, R.E., Salmon, E.D., Bement, W.M., 2000. Microtubules remodel actomyosin networks in Xenopus egg extracts via two mechanisms of F-actin transport. J. Cell Biol. 150, 361–376, (PMCID: PMC2180232).
Whitaker, M., 1996. Control of meiotic arrest. Rev. Reprod. 1, 127–135, (PMID: 9414449).
Yoshida, M., Sensui, N., Inoue, T., Morisawa, M., Mikoshiba, K., 1998. Role of two series of Ca2+ oscillations in activation of ascidian eggs. Dev. Biol. 203, 122–133. http://dx.doi.org/10.1006/dbio.1998.9037.
Yoshida, S., Marikawa, Y., Satoh, N., 1996. Posterior end mark, a novel maternal gene encoding a localized factor in the ascidian embryo. Development 122, 2005–2012, (PMID: 8681781).